# Equilibrium Geometries and Electronic Structure of Iron−Porphyrin Complexes: A Density Functional Study

**Carme Rovira,[†] Karel Kunc,[‡] Jürg Hutter,[†] Pietro Ballone,[†] and Michele Parrinello*,[†]**

*Max-Planck Institut für Festkörperforschung, Heisenbergstrasse 1, 70569 Stuttgart, Germany, and Laboratoire d'Optique des Solides, University Pierre et Marie Curie, 4 Place Jussieu, 75252 Paris-Cedex 05, France 10000*

*Received: July 8, 1997; In Final Form: August 11, 1997*[⊗]

We have performed density functional theory (DFT) calculations of iron−porphyrin (FeP) and its complexes with $O_2$, CO, NO, and imidazole (Im). Our fully optimized structures agree well with the available experimental data for synthetic heme models. Comparison with crystallographic data for proteins highlights interesting features of carbon monoxymyoglobin. The diatomic molecule induces a 0.3−0.4 Å displacement of the Fe atom out of the porphyrin nitrogen ($N_p$) plane and a doming of the overall porphyrin ring. The energy of the iron−diatomic bond increases in the order Fe−$O_2$ (9 kcal/mol) < Fe−CO (26 kcal/mol) < Fe−NO (35 kcal/mol). The ground state of FeP($O_2$) is an open shell singlet. The bent Fe−$O_2$ bond can be formally described as $Fe^{III}-O_2^-$, and it is characterized by the anti-ferromagnetic coupling between one of the d electrons of Fe and one of the $\pi^*$ electrons of $O_2$. FeP(CO) is a closed shell singlet, with a linear Fe−C−O bond. The complex with NO has a doublet ground state and a Fe−NO geometry intermediate between that of FeP(CO) and FeP($O_2$). The bending of the Fe−(diatomic) angle requires a rather low energy for these three complexes, resulting in large-amplitude oscillations of the ligand even at room temperature. The addition of an imidazole ligand to FeP moves the Fe atom out of the porphyrin plane toward the imidazole and decreases significantly the energy differences among the spin states. Moreover, our calculations underline the potential role of the imidazole ligand in controlling the electronic structure of FeP by changing the out-of-planarity of the Fe atom. The presence of the imidazole increases the strength of the Fe−$O_2$ and Fe−CO bonds (15 and 35 kcal/mol, respectively), but does not affect the energy of the Fe−NO bond, while the resulting FeP(Im)(NO) complex exhibits a longer and weaker Fe−Im bond.

## I. Introduction

Metal-substituted tetrapyrrole macrocycles, their complexes, and derivatives provide the active site (prosthetic group) for a large variety of biological enzymes. The importance of these molecules has motivated a vast research effort, whose results are collected in several books and recent review papers.[1] Of particular interest among these systems is the iron−porphyrin (FeP), which is closely related to the prosthetic group (the heme) of the oxygen-carrying proteins hemoglobin and myoglobin, and also of cytochrome *c* and peroxidase, i.e., two of the enzymes catalyzing important redox reactions in biological systems.[2]

Our study is focused on the complexation of FeP by small molecular ligands, relevant for the functioning of the heme group in hemoglobin and in myoglobin. It is well-known that the role of heme in these proteins is to bind reversibly an oxygen molecule. Although the chemical bond is localized in the immediate vicinity of the heme iron atom, the structure, stability, and chemical properties of the complex depend in an essential way on the protein environment. The same heme−protein interaction plays an important role in preventing the saturation of the prosthetic group by poisoning species, most notably CO.[3]

The structure of both hemoglobin and myoglobin is known with atomistic detail from X-ray studies of proteins.[4] Moreover, several features in the dynamics and electronic structure of heme have been investigated by infrared, Raman, Mössbauer, and ESR spectroscopy for crystal samples as well as for proteins in solution. A major impulse to the understanding of these systems has also been given by the synthesis of molecular models (see ref 1c for a recent review of the experimental information).

Despite all these studies, the clarification of the behavior of hemoglobin and myoglobin is still an elusive goal. In particular, it has proven very difficult to disentangle unambiguously the role of the short-range intraheme chemical interactions from the long-range heme−protein interactions on the structure and binding properties of of $O_2$, CO, and NO. A significant example of these uncertainties is provided by the recent debate on the mechanism by which hemoglobin and myoglobin discriminate against the binding of CO.[5] Understanding the chemistry of the isolated prosthetic group is the first step toward solving these issues, and theoretical studies could help to clarify the hypotheses that have been put forward by the experimental analysis.

Density functional studies have been reported for the gas-phase FeP.[6] Larger complexes have been modeled by simplified molecules or studied under restrictive assumptions on the geometry and/or the electronic structure. For instance, iron−porphyrin complexes with $O_2$, CO, and NO have been studied by means of semiempirical, Hartree−Fock, or Xα methods at fixed geometry,[7,8] usually taken from experiments. Those studies provided a useful picture of the bonding in these systems, although neither structural nor energetic data were quantitatively determined. Only a few post Hartree−Fock studies have been made on these systems,[9,10] although often at a fixed experimental structure, commonly taken from synthetic heme models. In particular, partial optimizations at the MP2 level using a limited basis set have been reported for a simplified FeP(Im)(CO) structure (Im = imidazole). It was concluded[10a] that the proximal histidine is responsible for a large distortion of the Fe−C−O unit. Recent density functional calculations by Ghosh et al.[10b] ruled out this conclusion and reported an estimate for the energy required to change the Fe−C−O angle in FeP(Im)(CO). It is worth mentioning that not all the ab initio methods

[†] Max-Planck Institut für Festkörperforschung.
[‡] University Pierre et Marie Curie.
[⊗] Abstract published in *Advance ACS Abstracts,* October 1, 1997.

S1089-5639(97)02211-1 CCC: $14.00 

have proved to be equally accurate in the study of metalloporphyrin derivatives. Hartree−Fock methods are known to favor high spin configurations, since they cannot account for the correlation energy.[6c] CI and CASSF calculations can be performed, but their computational cost precludes any structural relaxation.[9b,c] DFT-based methods, which account for the electronic correlation and are less demanding than the latter, have already proved to be very efficient in the calculation of similar iron complexes.[11,12] Among the DFT-based methods, the molecular dynamics of Car−Parrinello[13] has recently been applied with success to systems of biological interest,[14] including metalloporphyrin derivatives.[15] Here we apply this method to search for the minimum energy structures of the FeP and its $O_2$, CO, and NO complexes. The effect of an imidazole axial ligand is also analyzed, as a first step to investigate the effect of the local protein environment on the chemical properties of FeP. Altogether, our calculations provide a basis to understand the spin−structure relationships underlying the role of FeP as an active center in proteins.

## II. Computational Details

The Car−Parrinello method is described in detail by several publications.[13] Our computations are performed within the density functional framework,[16] with the local spin density[17] and gradient-corrected approximations for the exchange (Becke, 1986[18a]) and correlation (Perdew, 1986[18b]) energy. For reasons of numerical stability, gradient corrections (GC) are neglected where the density is lower than $5 \times 10^{-5}$ e/(au)$^3$. Tests with a different gradient correction formula (using the same Becke approximation for exchange, and the Lee, Yang, and Parr approximation for correlation[18c]) show only minor differences in the results presented below. Only valence electrons are explicitly included in our computation, and their interaction with the ionic cores is described by norm-conserving, ab initio pseudopotentials generated following the scheme of Troullier and Martins.[19] The angular nonlocality is taken into account by the Kleinman−Bylander construction.[20a] The pseudopotential for Fe is supplemented by nonlinear core corrections[20b] to enhance the transferability with respect to magnetic excitations.[21] Test computations on small-sized iron−$NH_3$ complexes were done to check the reliability of our approach. In agreement with other studies on iron complexes,[11] the spin contamination was found to be insignificant.

The molecules under study are enclosed in an orthorhombic box periodically repeated in space ($a = b = 15$ Å, $c = 8$ Å for the complexes without imidazole, $a = b = 15$ Å, $c = 11$ Å for the imidazole complexes). The importance of lateral interactions has been evaluated by a few computations with larger boxes: we verified that structure and binding energies of our complexes do not depend on the box size.

Single-electron Kohn−Sham (KS) orbitals are expanded in a plane wave basis, with a kinetic energy cutoff of 70−90 Ry. For the largest simulation cell we used, this corresponds to $7.2 \times 10^4$ plane waves per KS state and $6 \times 10^5$ plane waves for the density.

At fixed atomic position and for a given spin multiplicity of the molecule, the electronic ground-state energy is determined by direct minimization of the density functional expression with respect to the coefficient of the plane wave expansion for the electron orbitals.[22] For this optimization we used a combination of conjugate gradient[23a] and direct inversion in the iterative subspace.[23b]

The ground-state electronic density and Kohn−Sham eigenstates enter the computation of Hellmann−Feynman forces on the ions, which in turn, allow us to perform MD by a standard velocity Verlet algorithm. Molecular dynamics, with superimposed quenching or annealing, is used as an efficient strategy to optimize the molecular structures.[24,25] The resulting electronic configurations are analyzed by diagonalizing the Kohn−Sham Hamiltonian. Mulliken population analysis, atomic orbital contributions, and Mayer bond orders[26] are computed by projecting the KS orbitals on a minimal basis of atomic states.[27]

We briefly comment here on the importance of GC in our results. Geometry optimizations performed on FeP and its above-mentioned series of complexes but restricting ourselves to the local spin density (LSD) approximation for exchange and correlation show that there is an average expansion of ∼1%, on the average, in the LSD approximation (comparing with the experimental data). Binding energies, however, are overestimated by more than 100% (comparing with the LSD+GC results), although the same trend is predicted by both LSD and LSD+GC approaches. In the following we will base our discussion on the LSD+GC computations.

**TABLE 1: Calculated Minimum Structure (LSD+GC) for the Three Spin States of the Isolated Iron−Porphyrin. The $^3$FeP Structures Obtained in Previous DFT Studies Are Also Included, as Well as the Experimental Structure (X-ray) for the Iron−Tetraphenylporphine. Distances Are in Angstroms, Angles in Degrees, and Energies in kcal/mol**

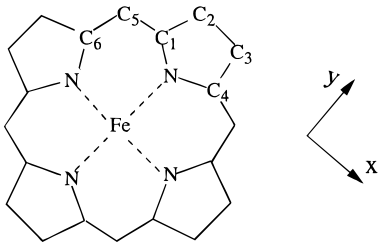


| parameter | $^1$FeP | $^3$FeP | $^5$FeP | $^3$FeP [6a] | $^3$FeP [6b] | $^3$FeTPP [28d] |
|---|---|---|---|---|---|---|
| Fe−N | 1.97 | 1.98 | 2.04 | 1.96 | 1.96 | 1.97 |
| N−$C_1$ | 1.39 | 1.39 | 1.38 | 1.38 | 1.37 | 1.38 |
| $C_1$−$C_2$ | 1.44 | 1.44 | 1.44 | 1.42 | 1.43 | 1.44 |
| $C_2$−$C_3$ | 1.36 | 1.36 | 1.36 | 1.36 | 1.36 | 1.33 |
| $C_1$−$C_5$ | 1.38 | 1.38 | 1.39 | 1.37 | 1.37 | 1.38 |
| $C_5$−$H_2$ | 1.09 | 1.09 | 1.09 | 1.10 | 1.09 | |
| $C_2$−$H_1$ | 1.09 | 1.09 | 1.08 | 1.09 | 1.09 | |
| ∠FeN$C_1$ | 127.8 | 127.6 | 126.8 | 127.9 | 127.6 | 127.3 |
| ∠N$C_1C_5$ | 125.1 | 125.3 | 125.2 | 125.1 | 125.4 | 125.1 |
| ∠N$C_1C_2$ | 110.8 | 110.7 | 111.3 | 111.2 | 110.6 | 110.2 |
| ∠$C_1C_2C_3$ | 106.9 | 106.9 | 107.2 | 106.7 | 106.9 | 107.1 |
| ∠$C_1C_5C_6$ | 124.2 | 123.8 | 125.9 | 123.9 | 124.2 | 123.5 |
| ∠$C_1C_2H_1$ | 124.4 | 124.2 | 124.6 | 124.4 | 126.3 | |
| ∠$C_1C_5H_2$ | 117.8 | 117.8 | 117.1 | 118.0 | 117.9 | |
| $E_{rel}$ | 12.7 | 0.0 | 14.7 | | | |

## III. The Isolated Iron−Porphyrin

The first part of our study is focused on the isolated FeP molecule, for which DFT computations have already been reported.[6a,b] For reasons of computational convenience, in these previous works the geometry optimization was done under the assumption of either $D_{4h}$ or $D_{2h}$ symmetry. Moreover, only the geometry of the ground state (spin multiplicity $M = 3$) was determined, the energy of other spin states being computed at the geometry of the ground state. To avoid any shortcomings due to these assumptions, our study will be performed without symmetry constraints and the structures corresponding to three different spin multiplicities ($M = 1$, 3, and 5) will be optimized.

We start our computation from the geometry of closely related metalloporphyrins reported in ref 15a, adding a slight out-of-plane displacement for the Fe atom (∼0.3 Å) and relaxing the structures at fixed spin multiplicity $M$. The distances and angles of the optimized geometries are collected in Table 1. The lowest

**SCHEME 1**

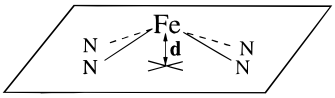


energy structure turns out to be a triplet ($M = 3$). The energies of the optimized $M = 1$ and $M = 5$ states (i.e., the adiabatic excitation energies to the lowest energy spin multiplicities) are also reported in Table 1.

Our results for the $M = 3$ ground state are in good agreement with those computed by DFT all-electron methods,[6a,b] thus showing that our pseudopotential plane wave scheme does not introduce any significant error. The energy differences among different spin states ($E_{rel}$) are lower than the ones previously reported, due to the fact that the structure of the $^5$FeP and $^1$FeP states was not optimized in these works.[6a,b] In the case of the high-spin state, the expansion of the Fe−$N_p$ distances with respect to the ground state results in a relatively large energy lowering (∼20 kcal/mol, comparing our results and those of ref 6a).

To our knowledge, no experimental data have been reported for the gas-phase FeP molecule. The closest comparison is with the crystal structure of Fe(II)−tetraphenylporphirin (FeTPP). Several experimental studies[28] have demonstrated that the ground state of the FeTPP molecule is a triplet, with bond distances (determined by X-ray diffraction[28d]) in good agreement with our results.

While our optimized structures for $M = 1$ and $M = 3$ are planar and have $D_{4h}$ symmetry,[29] the equilibrium position of the iron atom in $^5$ FeP is slightly ($d = 0.08$ Å) above the plane of the four nitrogen atoms (hereafter referred as the N-plane), resulting in a $C_{4v}$ symmetry (see Scheme 1). Computation of the energy as a function of Fe out-of-planarity results in two minima corresponding to a planar and a nonplanar structure, respectively. Nevertheless, the energy difference between both minima is only 0.2 kcal/mol, with an energetic barrier of the same magnitude. This energy gain associated with the Fe out-of-planarity is extremely small compared to the energy scale of almost any experimental probe, and the most apparent signature of the out-of-planarity is likely to be a highly anharmonic motion of Fe perpendicular to the porphyrin plane. It is a well-known empirical rule that high-spin states correspond to a large "atomic" radius for Fe, which could force it to go out of the plane.[2,30] Iron−nitrogen distances in the range 2.0−2.1 Å are common in crystals of high-spin FeP derivatives, while intermediate- and low-spin structures exhibit Fe−N distances in the range 1.9−2.0.[30] The computed Fe−N distances reported in Table 1 reflect the same trend. Remarkably, only the Fe−N distances are affected by the change in the spin multiplicity, underlining the rigidity of the porphyrin frame. In terms of the electronic structure, the expansion of the porphyrin core in the high-spin state ($^5$FeP) can be explained as a consequence of populating the antibonding $e_g^*$ molecular orbital (MO), which is mainly concentrated on the $d_{x^2-y^2}$ atomic orbital of the iron atom. This MO is, of course, not the only one that retains the atomic d orbital character; an analysis of the higher occupied MOs in each $^M$FeP ($M = 1, 3, 5$) structure reveals that the nature of these orbitals (i.e., as being of either metal or ligand character) is very well-defined. As a consequence, the number of electrons in molecular orbitals with d orbital character is a direct measure of the "formal charge" of the Fe atom, which allows us to describe the chemistry of the $^M$FeP spin states within the oxidation-state formalism.

As illustrated in Figure 1, six electrons can be associated with the Fe atom in the $^3$FeP state. Therefore, the Fe atom is in an

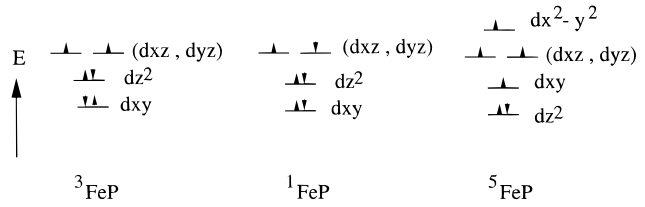


**Figure 1.** Schematic drawing of the orbital energy structure in the three lowest energy spin multiplicities of FeP.

**TABLE 2: Distribution of the Mulliken Charges among the Atoms or Groups of Atoms Building the Structures That Have Been Investigated. The Labeling of the Atoms Is Described in the Text**[a]

| structure | Fe | diatomic[b] | $N_p$ | $N_\epsilon$ |
|---|---|---|---|---|
| FeP | 0.98 | | −0.42 | |
| FeP(Im) | 1.04 | | −0.42 | −0.39 |
| FeP($O_2$) | 1.13 | −0.26 | −0.40 | |
| FeP(CO) | 1.06 | −0.08 | −0.40 | |
| FeP(NO) | 1.05 | −0.12 | −0.40 | |
| FeP(Im)($O_2$) | 1.19 | −0.35 | −0.39 | −0.37 |
| FeP(Im)(CO) | 1.04 | −0.06 | −0.38 | −0.36 |

[a] For a given structure, the listed values correspond to the lowest energy spin state. [b] $O_2$, CO, or NO.

oxidation state of 2 (i.e., $Fe^{II}$). Two additional facts reinforce this assignment. First, the chemistry of the closely related FeTPP molecule has also been described in terms of $Fe^{II}$. Second, a calculation of the charge on the Fe atom for the FeO molecule, which also contains a $Fe^{II}$, gives the same result as in the $^3$FeP spin state. The Mulliken populations of Fe and N in $^3$FeP are reported in Table 2. We point out that these values are not an absolute measure of the real charges on the atoms, since the charge distribution among them depends very much on the theoretical method one chooses. Nevertheless, the computed charges become useful when we compare trends among analogous molecules. As can be seen in Figure 1, the d electron configuration of Fe gives an electron count of six for all spin states. Consistently, the Mulliken charge on Fe remains constant upon changing spin multiplicity, and therefore, the Fe atom can be formally described as $Fe^{II}$ in all three spin states.

Analysis of the density distribution shows that, as expected, the spin density of the ground-state triplet is mainly localized on the Fe atom, with small pockets of opposite spin on the nitrogen atoms. The singlet is also an open shell system, the corresponding closed shell configuration being ∼3 kcal/mol higher in energy. We observe that, at variance from $M = 3$, the spin density is fully localized on Fe for $M = 1$ and $M = 5$.

## IV. The FeP Complex with $O_2$

As mentioned in the Introduction, binding and releasing one oxygen molecule is the major function of iron−porphyrin in hemoglobin and myoglobin. We optimize the structure of the FeP($O_2$) complex by a combination of relaxation and MD runs. The resulting structure is a spin singlet, with the $O_2$ molecule attached to the Fe ion in an angular configuration. This geometry, also found in several other complexes of transition metals with diatomic molecules, is commonly referred to as "end-on" (Scheme 2a). The computed binding energy of the FeP($O_2$) complex is 9 kcal/mol.

The interatomic distances and angles characterizing the ground-state structure are summarized in Figure 2 a. The FeP($O_2$) complex is of $C_s$ symmetry (the four Fe−N bonds, which are equivalent in FeP, split into two pairs of slightly different length, 1.99 and 2.02 Å). Because of the attraction by $O_2$, the

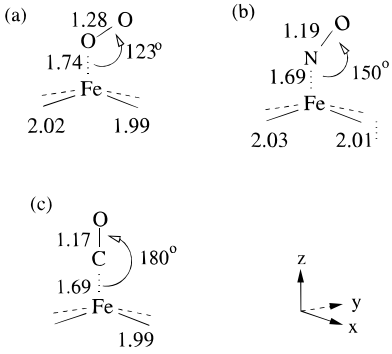


**Figure 2.** Geometry of the Fe−XY bond (X,Y = C, N, O) in the ground state of (a) $FeP(O_2)$, (b) FeP(NO), and (c) FeP(CO).

**SCHEME 2**


**2a** **2b**

Fe atom moves 0.3 Å out of the N-plane. This value is very similar to the ones observed in several 5-fold-coordinated transition metal complexes ($ML_5$), of which $FeP(O_2)$ is a typical example.[31] Outside this central core made by the Fe and N atoms, the porphyrin structure is almost unchanged upon complexation by $O_2$: only a limited "doming" (see Figure 3) with $D/R \approx 0.06$ is apparent in the ground-state geometry. The $O_2$ molecule itself, instead, appears to be more affected by the bonding to Fe: the computed O−O distance increases by ∼4% (from 1.23 Å in the isolated molecule to 1.28 Å in $FeP(O_2)$), while the Mayer bond order of O−O decreases from 1.4 to 1.3. These two observations suggest that electron charge is transferred from FeP to $O_2$, populating antibonding states and weakening the O−O bond. In the optimal structure, the projection of the O−O bond in the porphyrin plane lays along the bisection of one of the N−Fe−N angles, in the quadrant defined by the shortest Fe−N distances. The energy of the complex, however, changes only slightly (∼2 kcal/mol at most) by rotating the $O_2$ molecule around the Fe−O axis.

To the best of our knowledge, all the available experimental structures (determined by X-ray or neutron scattering) involving a $FeP(O_2)$ fragment concern crystals in which the octahedral position opposite $O_2$ is occupied by a nitrogenated ligand (imidazole, pyridine, or histidine, for instance). For this reason, the comparison of our structural results with experimental data is reported in section VII below.

The electronic structure of the $FeP(O_2)$ complex is particularly interesting: despite the $M = 1$ multiplicity, it is an open shell structure. The spin density distribution of this complex is displayed in Figure 4: the vanishing integrated spin density is the result of the anti-ferromagnetic coupling of two regions of opposite spin, centered on the Fe and on the oxygen molecule. The integrated spin density in each of these two regions is 0.88 electrons. This result is not unexpected, given the open shell nature of the interacting molecules and the relatively weak bond between them. Precisely on the basis of those two considerations, the anti-ferromagnetism of heme was already proposed by Weiss back in the 1960s.[32a] The Weiss picture, which describes the bonding as $Fe^{III}-O_2^-$, has been competing for many years with the picture proposed by Pauling,[32b] based on a $Fe^{II}-O_2$ scheme. Most of the experimental results for heme−proteins and synthetic models have been interpreted in terms of the Weiss description.[1c] On the theoretical side there is more

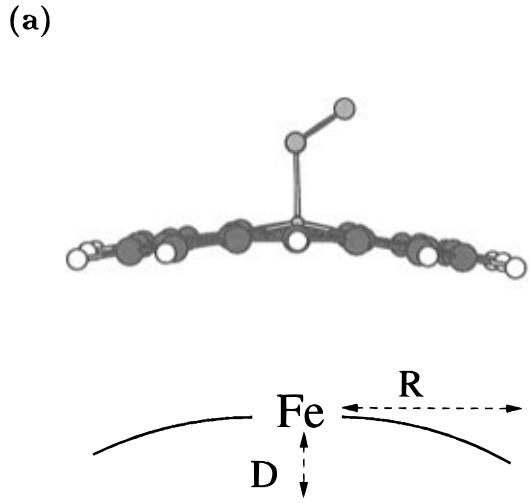


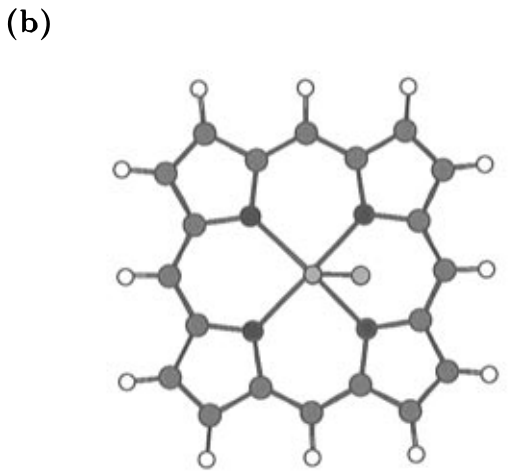


**Figure 3.** Optimized structure of the $FeP(O_2)$ complex. The domed shape of the porphyrin and the angular Fe−O−O structure can be visualized in the side view (a), while the top view (b) shows the O−O axis orientation with respect to the N-plane.

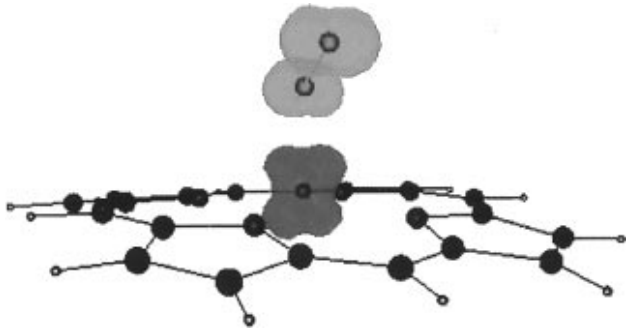

**Figure 4.** Unpaired spin density in the $FeP(O_2)$ ground state. The two surfaces centered on Fe (blue) and $O_2$ (red) enclose regions of opposite spin.

controversy,[7−9] since both models are supported by different computational schemes.

To describe the nature of the $Fe-O_2$ bonding in more detail, we analyze the higher occupied spin−orbitals of the $FeP(O_2)$ complex, and we classify them as being either of Fe, $O_2$, or porphyrin character (See Figure 5). The notation "P" is used to label the orbitals centered on the porphyrin ring. The indexes "s" and "a" are used to distinguish between the two $\pi_g^*$ orbitals of the $O_2$ molecule ($\pi_{g,s}^*$ is the orbital symmetric with respect to the plane of symmetry of the $FeP(O_2)$ complex and $\pi_{g,a}^*$ is

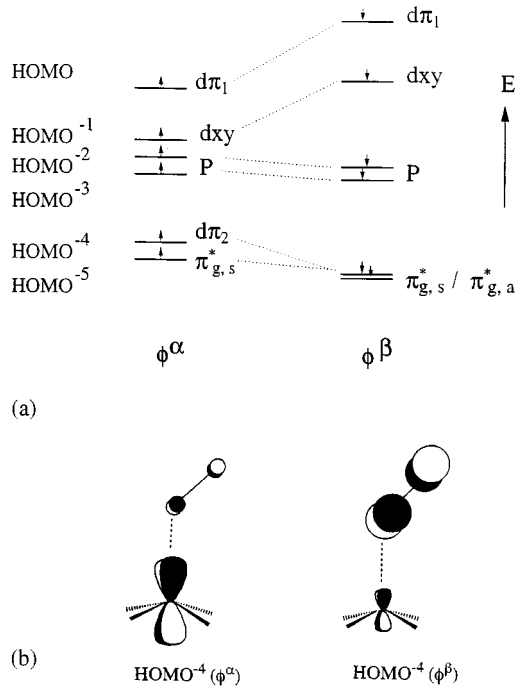


**Figure 5.** Relative energy and atomic orbital character of the higher occupied orbitals in the $FeP(O_2)$ complex. The α and $\beta$ labels refer to the spin up and down, respectively.

the antisymmetric one). The orbitals labeled as $d\pi_1$ and $d\pi_2$ refer to the $d_{xz}+d_{yz}$ and $d_{xz}-d_{yz}$ combinations, respectively, of the d orbitals of Fe (we follow the axes convention given in Table 1 and Figure 2). Only the $\pi^*_{g,a}$ orbital has the right symmetry to interact effectively with the $d\pi_2$ orbital of the Fe atom.

In order of decreasing energy, the first two orbitals (HOMO and $HOMO^{-1}$, with a total of four electron) are of Fe character. The next two orbitals ($HOMO^{-2}$ and $HOMO^{-3}$) are centered on the porphyrin. The orbital labeled as $HOMO^{-4}$ is the most interesting: the spin-up electron is on the Fe atom ($d\pi_2$), while the spin-down electron is on the $O_2$ molecule ($\pi^*_{g,a}$). This is precisely the orbital that contributes to the unpaired spin density, as can be seen by comparing Figure 4 with Figure 5b. Finally, the $HOMO^{-5}$ orbital is mainly the $\pi^*_{g,s}$ of the $O_2$ molecule (nevertheless, it also contains a small contribution of $d_{z^2}$). Thus, it is apparent that the total number of valence electrons that we can assign to the Fe atom is five and that there has been a transfer of one electron to the $\pi^*_{g,s}$ orbital of $O_2$. In fact, there has been a more complex electron rearrangement: of the two electrons in $d_{z^2}$, one has been transferred to one $d\pi$ orbital of Fe and the other to the $\pi^*_{g,s}$ orbital of $O_2$. This picture is consistent with the Mulliken population analysis, which shows an increase of the charge in Fe ($+0.2e$) with respect to the isolated FeP and a corresponding reduction of the charge on $O_2$ ($-0.3e$, see Table 2). Therefore, our results support the Weiss description for the $Fe-O_2$ bond (i.e., $Fe^{III}-O_2^-$).

It is interesting to compare our first-principles description of the $Fe-O_2$ bond with the model proposed by Hoffmann et al. in the late 1970s,[8] in which the authors rationalized the geometry of the $Fe-O_2$ bond in terms of the lower d-block levels of the metal atom and the frontier orbitals of the diatomic molecule. According to ref 8, the orbital originating from the antibonding combination of the $d_{z^2}$ orbital of Fe and the $3\sigma_g$ orbital of the $O_2$ molecule (referred to as "$z^2-n$" in ref 8) is likely to be the HOMO in a linear Fe−O−O conformation. However, its energy has a minimum as the $O_2$ molecule bends, which turns out to be the factor that leads the diatomic to adopt a bent Fe−O−O geometry. This corresponds very well with what we observe in our computations, the "$z^2-n$" orbital being the $HOMO^{-5}$ orbital of Figure 5. The only difference is that, in our case, the $d_{z^2}$ character of this orbital is considerably reduced in the bent $FeO_2$ structure. However, by deforming the Fe−O−O bond toward the linear geometry, we observe an increase in the $d_{z^2}$ character, as well as an increase in its relative energy (it becomes the HOMO). At the same time, the total energy of the $FeP(O_2)$ increases so much that the complex is no longer bound. Thus, the relative energy of the "$z^2-n$" orbital appears to be an important factor governing the geometry of the $FeO_2$ moiety.

Low-temperature infrared (IR) and resonant Raman (RR) studies[33] on the co-condensation of Fe(TPP) with $O_2$ (at 15 and 30 K, respectively) have shown that, besides the ground-state *end-on* geometry, the $O_2$ molecule can bind to Fe through both oxygen atoms, in the so-called *side-on* geometry (see Scheme 2b). This type of linkage to Fe is also found in dioxygen complexes of other 3 d transition metals, like Ti or Co.[34] The side-on isomer is less stable than the end-on, and it converts to the latter when the temperature is raised to 110 K.[33] The two isomers are distinguished experimentally by the O−O stretching frequency (a band at 1188−1223 $cm^{-1}$ for the *end-on* and at 1102−1105 $cm^{-1}$ for the *side-on*[33b]). Despite that the *side-on* isomer is undoubtedly present in the low-temperature Fe(TPP)-$(O_2)$ system, our efforts to optimize this structure have been unsuccessful. Starting from a geometry close to the one depicted in Scheme 2b and performing a quenched MD simulation, the lowest energy spin structure turns out to be the triplet $^3FeP-(O_2)$. However, this structure is unstable with respect to the dissociation in $^3FeP$ and $^3O_2$ moieties, it evolves toward the *end-on* structure if the system is annealed, and the spin is allowed to adjust to $M = 1$. This discrepancy with the experimental results might be due to the fact that the FeTPP molecule (on which the experiments are based) contains four phenyl side groups. The ruffling of the porphyrin, caused by the phenyl groups, could affect the delocalized $\pi$ orbitals in the aromatic ring and change slightly the chemical properties of the molecule such as to provide a weak binding for the *side-on* complex. However, we suspect that the discrepancy is due to the fact that the bond is very weak, due mainly to van der Waals forces, which are not present in our semilocal DFT scheme. This interpretation is supported by the fact that the temperature at which the experimental system reverts to the ground-state *end-on* geometry is very low (110 K).

Having determined the ground-state structure, we turn briefly to dynamical properties. The most investigated vibrational property of dioxygen FeP complexes is the $O_2$ stretching frequency, which is accessible by infrared and Raman spectroscopy.[33] This mode provides a sensitive probe of the diatomic electronic configuration, since the $O_2$ molecule is bound only weakly to the heavier Fe atom, and it is therefore relatively uncoupled to the porphyrin vibrations.[35] This last property allows us to compute easily the O−O stretching frequency. First, we determine the total energy $E$ of the system while constraining the O−O distance at a few values within a narrow interval (±3%) around the equilibrium value. For each of these distances we compute the total energy of the system, while optimizing all the other degrees of freedom (it is to be noted however that both the structure and the total energy of the complex change very little after the optimization). We estimate the stretching frequency by a least-squares fit of $E$(O−O) with a parabola. The calculated value for $\nu_{OO}$, 1222 $cm^{-1}$, agrees well with the experimental range of 1188−1223 $cm^{-1}$ determined for Fe(TPP).[33b] The close agreement is partly

**TABLE 3: Frequencies Corresponding to the Stretching Mode of the Diatomic Molecule ($O_2$ or CO) in the Complexes Investigated. The Value for the Isolated Diatomic Is Also Included, To Allow Comparisons**

| | calculated | | experimental | |
|---|---|---|---|---|
| structure | O−O (Å) | $\nu_{OO}$ ($cm^{-1}$) | O−O (Å) | $\nu_{OO}$ ($cm^{-1}$) |
| $^1FeP(O_2)$ | 1.28 | 1222 | | 1188−1223[33b] |
| $^1FeP(Im)(O_2)$ | 1.30 | 1046 | 1.2−1.3[44] | 1160[1c] |
| $^2O_2^-$ | 1.34 | 1076 | 1.30[34] | 1146[34] |
| $^3O_2$ | 1.23 | 1651 | 1.21[48] | 1580[48] |
| structure | C−O (Å) | $\nu_{CO}$ ($cm^{-1}$) | C−O (Å) | $\nu_{CO}$ ($cm^{-1}$) |
| $^1FeP(Im)(CO)$ | 1.17 | 1789 | 1.12−1.16[39] | 1940−1980[47] |
| $^1CO$ | 1.14 | 2082 | 1.13[48] | 2170[48] |

**SCHEME 3**

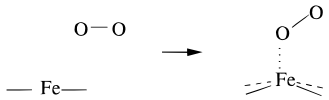


fortuitous, since the DFT−GC computation of frequencies is affected by systematic errors. The global uncertainty of our results is of the order of 5%, as can be estimated from Table 3, comparing the computed and experimental values of the stretching frequencies for the free $O_2$ molecule and the superoxide anion ($O_2^-$). This error bar is comparable to that of previous DFT−GC computations.[36] In agreement with the experimental evidence, our results show that the formation of the Fe−$O_2$ bond decreases the strength of the O−O bond.

As a last point, to get a glimpse of the finite temperature dynamics of complexation, we perform a short constant energy MD simulation of this reaction, again with the global spin multiplicity fixed at $M = 1$. We start from the equilibrium geometry of $^3$FeP, and we add the $O_2$ molecule above the porphyrin plane, at a distance within the range ∼3.0−3.5 Å. The $O_2$ molecule moves toward the Fe atom and attaches in the *end-on* position (see Scheme 3) in a very short time (200 fs). Our results suggest that there is no significant energy barrier associated with the reaction in the gas phase.

## V. The FeP Complex with CO

The complexation of FeP with CO has been studied with a procedure similar to the one used for $FeP(O_2)$. The ground-state FeP(CO) is a closed shell singlet, with a binding energy of 26 kcal/mol, i.e., almost 3 times larger that that of $FeP(O_2)$.

The ground-state geometry is summarized in Figure 2c. The most apparent difference with respect to the previous complex is that the Fe−C−O angle is linear. Despite the stronger binding, and the small size of the C atom, the Fe−C bond length (1.69 Å) is only slightly shorter than the Fe−O one in $FeP(O_2)$ (1.74 Å). The porphyrin ring has a domed geometry, as in the case of the $FeP(O_2)$ complex. The displacement of the Fe atom with respect to the N-plane amounts to 0.3 Å. The Fe−N distances expand with respect to $^3$FeP, although less than in the $FeP(O_2)$ complex.

The electronic structure of the FeP(CO) complex shows significant differences with respect to the $O_2$ complex. Starting from the highest occupied MO and in order of decreasing energy, there are three orbitals with a clear Fe character: $d_{xy}$ (HOMO), $d_{yz}$ (HOMO$^{-1}$), $d_{xz}$ (HOMO$^{-2}$). Thus, six electrons can be assigned to the Fe atom, which is formally described as $Fe^{II}$. This assignment is consistent with the fact that the Mulliken charges on the C and O atoms (and therefore the total charge on FeP) do not change with respect to the isolated molecule. The reason for a linear Fe−C−O angle can be traced

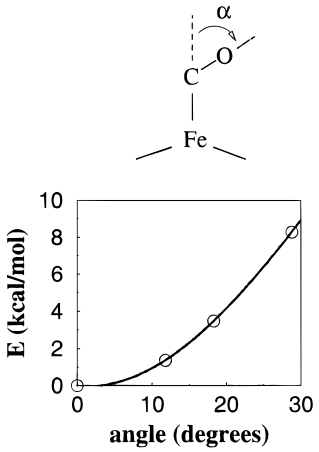


**Figure 6.** Energy ($E$) required to bend the Fe−C−O angle.

back to the electronic structure: this geometry allows a maximum Fe−CO $\sigma$-bonding (the interaction between the $d_{z^2}$ orbital of Fe and the $3\sigma_g$ orbital of CO), as well as a more effective $\pi$-back-bonding (i.e., the interaction of $d_{yz}$ and $d_{xz}$ with the empty $\pi_g^*$ orbitals of CO). In the $FeP(O_2)$ case, by contrast, there are two additional electrons which, as mentioned before, occupy the "$z^2-n$" level and give rise to a strong tendency toward the bent structure. This picture suggests that the FeP(NO) complex, which has only one electron more than FeP(CO), would adopt a structure intermediate between FeP(CO) and $FeP(O_2)$ (see section VI below).

The bending of the Fe−CO angle in hemoglobin and myoglobin has often been discussed in connection with the selective suppression of the CO binding in these proteins.[3,5] To compute the energy change associated with a nonlinear Fe−CO bond, we relax the FeP(CO) complex by constraining the nonlinearity of the Fe−C−O angle (α) at several different values in the interval α [0−30°]. The corresponding energy variations are reported in Figure 6. It can be appreciated that, up to ∼15°, the bending energy is very small. Given the fact that the angle of deviation measured experimentally is within this range (approximately 11° according to the recent X-ray structure of MbCO[4d] and less than 7° according IR experiments in solution[37]), it is unlikely that a slight Fe−C−O bending has a significant effect on the protein affinity for CO.[38] In fact, thermal energy alone (∼0.5 kcal/mol) can easily account for small deviations of the Fe−C−O angle from linearity. This picture suggests factors other than the CO bending are likely to control the affinity for CO in the protein. In this respect, it is worth mentioning that recent RR studies[39d] have underlined the importance of distal polar interactions in the heme pocket. On the other hand, it has been pointed out that for a large class of wild and mutant myoglobin and hemoglobin crystals the Fe−CO geometry and CO affinity are not highly correlated.[40]

Similarly to what we found for $FeP(O_2)$, we observe that, for a bent Fe−C−O unit, the energy is rather insensitive to rotations of the CO molecule around the Fe−*C* axis. This explains why in hemoglobin and myoglobin crystals the orientation of CO parallel to the heme plane displays a significant degree of disorder.

Our results for the FeP(CO) geometry and Fe−CO bending energy are in fair agreement with those reported in ref 10b, computed by a similar DFT scheme. The small differences between the two results are probably due to (i) the different exchange−correlation approximation (LDA in ref 10b, but including gradient corrections in our computation) and (ii) a different degree of geometry optimization: for each value of the Fe−C−O angle we fully relaxed all the remaining degrees

of freedom, while the optimization was restricted to the Fe−C−O bond in ref 10b.

### VI. The FeP Complex with NO

Despite the importance of the nitrosyl−heme complex, only a few computations at the semiempirical level have been reported in the literature for FeP(NO).[7d−f] In our study, we analyze the $M = 2$ and $M = 4$ spin multiplicities of this complex. In both cases we start from the optimized geometry of FeP($O_2$), we replace the oxygen closest to Fe by nitrogen, and we let the system relax. The ground state has a multiplicity $M = 2$, with a binding energy of 35 kcal/mol with respect to $^3$FeP and $^2$NO. The $M = 4$ multiplicity is 15 kcal/mol higher than the ground state, and therefore, it is also bound. Among the pentacooordinated complexes we considered in our study, FeP(NO) is the only one being significantly bound in more than one spin multiplicity.

The equilibrium geometry of the $M = 2$ ground state is illustrated in Figure 2b: the NO is attached in the "end-on" configuration, and the complex has $C_s$ symmetry. The structural features of this molecule are rather similar to those of FeP($O_2$), and as discussed below, they have a similar origin in terms of the electronic structure. At equilibrium the NO molecule lies in the plane bisecting one of the N−Fe−N angles of FeP and resides in the smallest of the four N−Fe−N quadrants. The energy associated with rotations of NO with respect to the Fe−N axis is small, comparable to the one we computed for FeP($O_2$) and FeP(CO) (∼2 kcal/mol). The Fe−N bond length (1.69 Å) is shorter than Fe−O in FeP($O_2$) and equal to Fe−C in FeP(CO), consistently with the fact that the Fe−NO bond is the strongest among these complexes. The strength of the Fe−NO bond is reflected also in the expansion of the Fe−N distances in the porphyrin plane and in the out-of-planarity of the iron atom ($d = 0.36$ Å), which are larger than in the other FeP(XY) complexes. The interatomic distance of NO expands by ∼2% upon complexation.

A long-standing problem has been the spatial distribution of the unpaired spin density: detailed electron paramagnetic resonance (EPR) studies[41] have been unable to determine unambiguously the partition of the spin density between the iron and the NO ligand. Our computation shows that in the ground state the spin density is localized mainly on the iron ion, which in turn can be regarded as being in a doublet spin state. Residual spin density is located on NO, but it has zero integral: an almost sinusoidal spin wave resides on NO, with both the N and O atom having polarization opposite to that of Fe, and a compensating spin density in the middle of the NO bond (See Figure 7).

The analysis of the higher occupied MOs of $^2$FeP(NO) shows that the unpaired electron of the FeP(NO) complex comes from the HOMO orbital, which is mainly given by the $d_{z^2}$ orbital of Fe, with a small contribution of the orbitals of NO. This HOMO orbital corresponds to the "$z^2-n$" level of the Hoffman model described before. The partial occupancy of this level leads to a geometry that is intermediate between that of the CO and $O_2$ complexes. In fact, the Fe−NO angle we obtain (150°) is almost exactly the arithmetic average of the Fe−CO (180°) and Fe−$O_2$ (121°) angles. The energy required to bend the Fe−N−O angle is very small: 4.5 kcal/mol is sufficient to change this angle from the equilibrium value (150°) to 180°.

Unlike the $O_2$ and CO cases, the d orbitals of Fe are now strongly mixed with the $\pi_g^*$ orbitals of NO. This situation is not unexpected, given the fact that the energy of the $\pi_g^*$ orbitals decrease along the sequence: CO > NO > $O_2$. In the two extreme cases, i.e., FeP($O_2$) and FeP(CO), the $\pi_g^*$ orbitals are well separated in energy (below and above, respectively) from the d orbitals of Fe, and thus each orbital retains mostly its character upon complexation. In contrast, the d orbitals of Fe lie close to the $\pi_g^*$ orbitals of NO, which results in a strong orbital mixing in the FeP(NO) complex. As a consequence, it is not possible to assign an oxidation state to the iron atom and a formal charge to the FeP and NO moieties by a simple inspection of the molecular orbitals. Nevertheless, the analysis of other structural and electronic properties might suggest a description of the bond in terms of $Fe^{III}-NO^-$. These properties are the distances among Fe and the nitrogens in the porphyrin ($Fe-N_p$), which are close to those of FeP($O_2$), the N−O distance (1.19 Å), which expands with respect to the free molecule (1.17 Å), and the fact that the unpaired electron is localized on Fe. The computed Fe−N−O angle ($\Theta = 150°$) is in good agreement with the one measured for the FeTPP(NO) crystal structure ($\Theta = 149°$), determined by X-ray diffraction.[42a] The other bonding parameters provided by the computation also agree fairly well with those reported in ref 44a. The main disagreement appears to be in the N−O distance. Our simulation gives $R$(N−O) = 1.19 Å, while the experimental separation is $R$(N−O) = 1.12 Å.[42a] Because this value is shorter than the experimental distance for an isolated NO molecule (1.15 Å),[43] we suspect that the N−O distance of the crystal structure is largely underestimated. The only alternative explanation for the discrepancy could be that in FeTPP(NO) the bond is of $Fe^{II}-(NO)^+$ type, since $NO^+$ has a bond length shorter than NO,[43] instead of $Fe^{III}-NO^-$ type, as found in the calculation. However, the good agreement between computations and experiment for all the other structural parameters suggests that this explanation is rather unlikely.

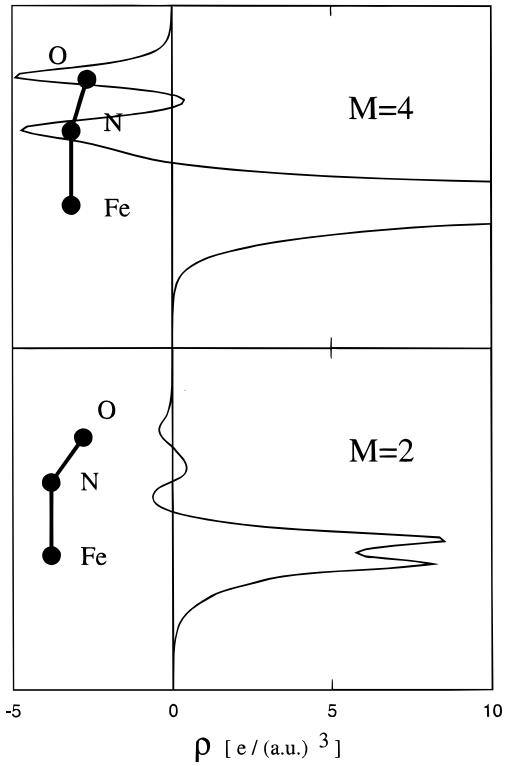


**Figure 7.** Spin density of the FeP(NO) complex averaged along planes parallel to the porphyrin ring for the two bound spin states of the complex ($M = 4$ and $M = 2$).

The $M = 4$ spin multiplicity has an "end-on" geometry similar to the $M = 2$ one; however, there are few characteristic differences: (i) The distance between Fe and the N of NO is slightly longer (1.72 Å) for $M = 4$ than for $M = 2$, presumably because of the reduced binding of the complex. Nevertheless,

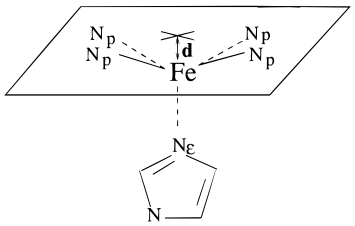


**Figure 8.** Geometric parameters we use to describe the structure of the FeP(Im) complex.

this distance remains much shorter than the Fe−$N_p$ distances. (ii) The Fe out-of-planarity ($d$ = 0.55 Å) is the largest among the complexes that we have studied, and the Fe−$N_p$ distances (2.11 Å) are much longer than in the $M$ = 2 ground state. (iii) The N−O distance decreases slightly (N−O 1.18 Å), suggesting that electronic charge is flowing back from NO to FeP. (iv) The Fe−N−O angle increases, being now almost linear ($\Theta$ = 172°). Analysis of the charge and spin density (see Figure 7) suggests that the $M$ = 4 species is the result of the antiferromagnetic coupling between a quintuplet FeP and a doublet NO (the integrated spin density on the FeP and NO fragments amounts to four and one electrons, respectively). Therefore, the FeP(NO) complex can be regarded as given by a weak bonding of an almost unperturbed $^2$NO molecule with $^5$FeP.

## VII. The Effect of an Imidazole Ligand

As a first step in understanding the role of the protein environment on the heme group, we study the influence of a nitrogenated axial ligand on the structure and bonding properties of the above systems. Our objective is to analyze the role of the proximal histidine, the basal ligand of heme in both hemoglobin and myoglobin. In analogy with what has been done in synthetic heme models such as the "picket-fence",[44] we attach an imidazole molecule (Im) to the iron atom via the $N_\epsilon$ nitrogen (see Figure 8). Although simpler, the imidazole contains all the basic elements of the histidine residue.

**The FeP(Im) Complex.** The structural and energy changes induced by the imidazole on the isolated FeP are summarized in Table 3. The structural changes are similar to those observed upon the complexation of FeP by $O_2$ or CO: the Fe atom moves out of the N-plane toward the imidazole, as depicted in Figure 8, and changes the relative energy among the spin states. The quintuplet state becomes significantly close (6.5 kcal/mol) to the ground triplet state. The porphyrin frame is slightly domed, although less than what we found for the $O_2$ and CO complexes. We observe that the energy of FeP(Im) does not depend significantly on the orientation of the imidazole plane with respect to the porphyrin. The reduction of the low lying excitation energies is the most important effect induced by the Im ligand on FeP and could have important consequences for biological processes. As apparent from the results of the previous sections, the reaction of FeP with the diatomics may require the change of the spin multiplicity to reach the ground state of the final complex. By changing the energy associated with this process, the Im ligand could alter drastically the kinetics of the reactions involving FeP.

The FeP(Im) complex shows a very interesting spin−structure relationship. As apparent from Table 4, the iron out-of-planarity ($d$) depends on the spin multiplicity: it is 0.24 Å for the singlet, 0.15 Å for the triplet, and 0.33 Å for the quintuplet. This suggests that the relative stability of the different spin states can be influenced by small structural distortions in the Fe−Im geometry and, in particular, by variations in the iron out-of-planarity. We verified that this is indeed the case by computing the adiabatic spin excitation energies for several values of $d$.

**TABLE 4: Energy with Respect to the Ground State ($E_{rel}$), Fe−N Distances, and Out-of-Planarity of the Iron Atom ($d$, As Described in Figure 3) Corresponding to the Lowest Lying Spin States of FeP(Im). Energies Are Given in kcal/mol and Distances in Angstroms[a]**

| spin−structure | $E_{rel}$ | Fe−$N_p$ | $d$ | Fe-$N_\epsilon$ |
|---|---|---|---|---|
| $^1$FeP(Im) | 8.3 | 1.99 | 0.24 | 1.99 |
| $^5$FeP(Im) | 6.5 | 2.04 | 0.33 | 2.10 |
| $^3$FeP(Im) | 0.0 | 2.00 | 0.15 | 2.14 |

[a] Notation: $N_p$ = porphyrin nitrogen. $N_\epsilon$ = imidazole nitrogen coordinated to the Fe atom. $d$ = distance of the Fe atom to the mean plane defined by the four $N_p$ atoms.

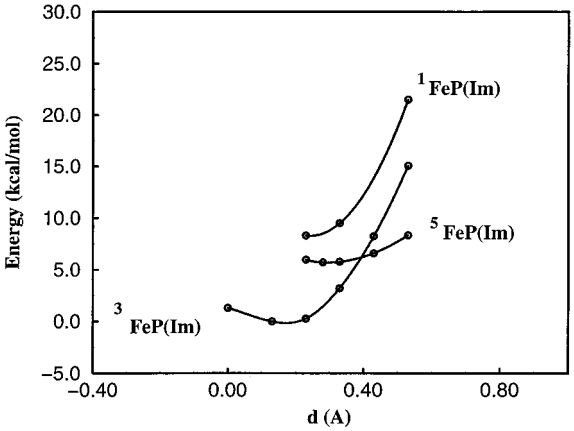


**Figure 9.** Energies of the $M$ = 1, 3, and 5 spin multiplicities of $^M$FeP(Im) as a function of the displacement of the iron atom ($d$) with respect to the N-plane.

The results are reported in Figure 9. Each curve is computed by constraining the nitrogen atoms to lie in a plane, with the Fe atom at a fixed height $d$ below it (see Figure 8). All the other degrees of freedom are optimized. The results confirm that the relative energy of the different spin multiplicities depends strongly on the structural parameter $d$. In particular, a large value of $d$ (>0.4 Å) stabilizes the quintuplet state versus the lower spin multiplicities. This spin−structure relation could have important implications in the chemistry of heme−proteins. It is worth mentioning that several experiments have demonstrated that the deoxy form of both myoblobin and hemoglobin, where the iron atom lies ∼0.42−0.63 out of the N-plane, is in a high-spin ground state.[1c] Our results highlight the ability of the imidazole ligand in controlling the electronic structure of the FeP, which could provide an easy mechanism for the protein to prepare the active center in the most useful spin multiplicity.

**The FeP(Im)($O_2$) and FeP(Im)(CO) Complexes.** We now turn to the FeP(Im)($O_2$) and FeP(Im)(CO) complexes. In both cases the ground state is a spin singlet. The resulting binding energies are 15 and 35 kcal/mol, respectively. These values are significantly higher than those computed without the imidazole ligand, the relative increase being more important for the $O_2$ complex.

Despite the stronger interaction of the diatomic with the rest of the complex, the $O_2$ molecule can still rotate around the Fe−O axis without significant energy barriers, and the Fe−C−O angle can also be changed at little cost in terms of energy. The Fe−C−O bending energy, in particular, seems to be slightly lower in the presence of Im than without, although the difference is hardly significant.

The electronic structure of FeP(XY)(Im) (XY = $O_2$, CO) is very similar to that of FeP(XY). In particular, the analysis of the spin density for FeP(Im)($O_2$) reveals a picture very similar to the one obtained for FeP($O_2$): the system is an open shell singlet, with two regions of opposite spin located on Fe and

$O_2$. The integrated spin in each of these two regions is 0.88*e*, i.e., equal to the one in $FeP(O_2)$. Nevertheless, we point out that the corresponding closed shell singlet of the $FeP(Im)(O_2)$ complex (described as $Fe^{II}(S=0)-O_2(S=0)$) lies only 3 kcal/mol higher than the open shell ground state. This small energy difference is likely to be affected by the protein environment, where a small perturbation (a distortion of the heme structure, the electrostatic field of the protein, or spin−orbit coupling) could lead to a mixing of the two states. Therefore, both situations are predicted to be possible once heme−protein interactions are taken into account. A polarity in the Fe−O bond, as present in the open shell state, would reinforce the hydrogen bond to the distal histidine (Fe−O−O···H−N), which in turn would favor $O_2$ binding versus CO. A nonpolar bond, on the other hand, could be useful in the mechanism of $O_2$ release from the heme pocket.

The strengthening of the $Fe-O_2$ and Fe−CO bonds upon inclusion of imidazole can be easily explained in terms of the changes in the main orbital interactions. The main contribution to the binding in the FeP(Im)(XY) complexes originates from the $\sigma$-bonding interaction between the low lying $3\sigma_g$ orbital of the diatomic molecule and the $d_{z^2}$ orbital of the Fe atom. To understand the changes in the $3\sigma_g-d_{z^2}$ interaction induced by Im, it is useful to look at the complexation in two steps: (i) the binding of Im to FeP and (ii) the binding of the diatomic to the resulting FeP(Im) complex. In the first step, the direct effect of Im on the electron distribution of FeP consists in polarizing the $d_{z^2}$ orbital out of the FeP plane, toward the remaining vacant ligand position. This makes the $d_{z^2}$ orbital better prepared to interact, in the second step, with the $3\sigma_g$ orbital of the diatomic. As a result, the overlap between $d_{z^2}$ and $3\sigma_g$ increases, which in turn contributes to the strengthening of the bond.

The optimized structure of the $FeP(Im)(O_2)$ complex is reported in Figure 10, and Table 5 contains the most relevant structural information about the complexes analyzed. The simultaneous presence of Im and the diatomic molecule XY (XY being $O_2$ or CO) gives rise to an approximate octahedral coordination shell for Fe and restores the planarity of the $FeN_4$ fragment. The Fe−N distances within the porphyrin expand further, but this effect is less important than upon the first axial coordination. The Fe−XY binding geometry depends slightly on the presence of Im: the Fe−X distance increases (by 2% in both the $O_2$ and CO complexes) despite the increase in the bond strength. The CO distance remains constant and the O−O distance increases by 2%, suggesting that additional charge is transferred to $O_2$.

The overall structure of $FeP(Im)(O_2)$, and especially the geometry of the $Fe-O_2$ bond, are close to the X-ray structures determined for both synthetic iron−porphyrin−imidazole complexes and heme−proteins. For instance, in the "picket-fence" model, [Fe(TpivPP)(1-MeIm)($O_2$)], the main structural parameters are Fe−O = 1.75(2) Å, O−O = 1.2(1) Å, $Fe-N_p$ = 1.98(2) Å, Fe−O−O= 131(2)°,[44] while in myoglobin they are Fe−O = 1.83 Å, O−O = 1.22 Å, $Fe-N_p$ = 1.90−2.00 Å, Fe−O−O = 115.5°.[4g] Consistently with our observation that $O_2$ can rotate almost freely around the Fe−O axis, the experimental results show that the projection of the O−O bond in the porphyrin plane is different in different environments: in the picket-fence it lies in the plane bisecting one of the N−Fe−N angles, while in myoglobin and hemoglobin the projection of the $O_2$ molecule nearly overlaps with one of the Fe−N bonds. Apparently, even a small perturbation due to the protein environment (for instance a hydrogen bond with the distal histidine) is sufficient to rotate the equilibrium position of $O_2$ around the Fe−O axis.

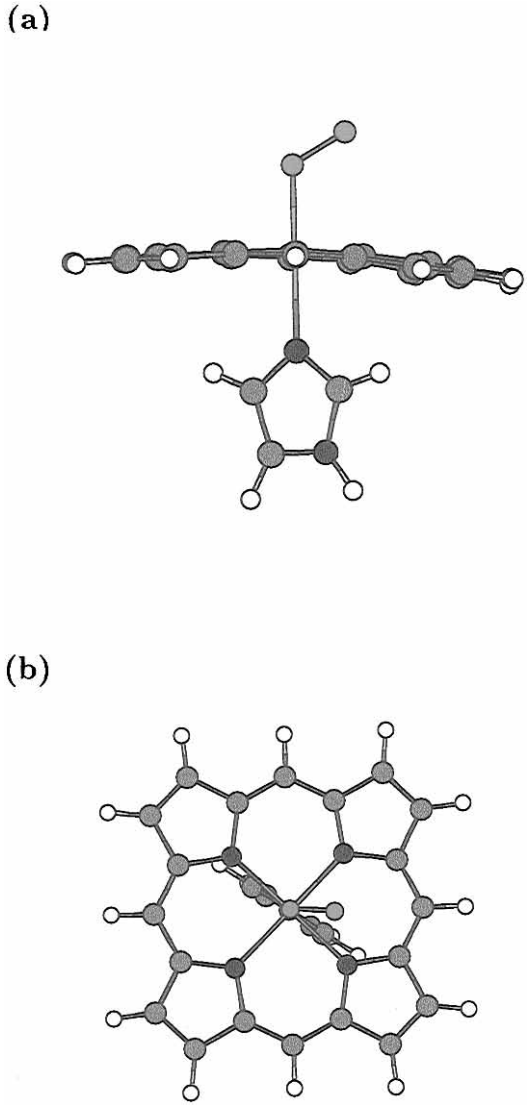


**Figure 10.** Ground-state geometry of the $FeP(Im)(O_2)$ complex: (a) side view; (b) top view showing the orientation of the O−O axis and the imidazole plane with respect to the N-plane.

Experimental X-ray data for the FeTPP(py)(CO) complexe (py = pyridine) and other synthetic heme models[39] consistently give Fe−(CO) bond lengths in the range 1.74−1.77 Å, and C−O separations between 1.12 and 1.16 Å, i.e., close to the equilibrium parameters obtained in our computation for FeP-(Im)(CO). The comparison with experimental data for carbon monoxymyoglobin crystals is more intriguing: here Fe−CO distances in excess of 1.85 Å are measured by X-ray and neutron diffraction,[4b−e] and the discrepancy with our results is beyond the uncertainties of both the experiments and our model. Together with the fact that for $FeP(O_2)(Im)$ our computation gives a $Fe-(O_2)$ distance closer to the experimental one even for proteins, these observations suggest that, in the case of CO in myoglobin, an additional *long-range* force is superimposed on the short-range chemical interactions.

Unfortunately, there is little direct experimental information on the specific effects of the Im ligand on the stability of the FeP(XY) complexes. Nevertheless, it is known that the stretching frequency of $O_2$ in gas-phase iron−porphyrin complexes decreases in the presence of an axial base ligand.[33] This experimental observation is taken as an indication of a strengthening of the Fe−O bond, which is consistent with our results. For a more direct comparison between our results and the experimental data, we computed the stretching frequency of $O_2$

**TABLE 5: Computed Structure and Binding Energy of the FeP(AB) and FeP(Im)(AB) Complexes Investigated (AB = $O_2$, CO, NO). Distances Are in Angstroms, Angles in Degrees, and Energies in kcal/mol. The Experimental Values Correspond to X-ray Structures of Heme Models[39a,42,44]**

| structure | | Fe−A | A−B | ∠Fe−A−B | Fe−N | Fe−$N_\epsilon$ | $\Delta E$ |
|---|---|---|---|---|---|---|---|
| $^1$FeP(CO) | calc | 1.69 | 1.17 | 180 | 1.99 | | 26 |
| | expt | 1.77(2) | 1.12(2) | 179(2) | 2.02(1) | 2.10(1) | |
| $^2$FeP(NO) | calc | 1.69 | 1.19 | 150 | 2.03−2.01 | | 35 |
| | expt | 1.71(1) | 1.12(1) | 149(1) | 2.00 | | |
| $^1$FeP($O_2$) | calc | 1.74 | 1.28 | 123 | 2.02−1.99 | | 9 |
| | expt | 1.75(2) | 1.2(1) | 131(2) | 1.98(2) | 2.07(2) | |
| $^2$FeP(Im)(NO) | calc | 1.72 | 1.20 | 138 | 2.02−2.01 | 2.22 | 36 |
| | expt | 1.74(1) | 1.12(1) | 140 | 2.01(1) | 2.18(1) | |
| $^1$FeP(Im)(CO) | calc | 1.72 | 1.17 | 180 | 2.02 | 2.07 | 35 |
| | expt[a] | 1.77(2) | 1.12(2) | 179(2) | 2.02(1) | 2.10(1) | |
| $^1$FeP(Im)($O_2$) | calc | 1.77 | 1.30 | 121 | 2.02−2.01 | 2.08 | 15 |
| | expt[b] | 1.75(2) | 1.2(1) | 131(2) | 1.98(2) | 2.07(2) | |

[a] The experimental model[39a] contains pyridine as an axial ligand instead of imidazole. [b] The O−O bond distance of the crystal structure is highly imprecise.

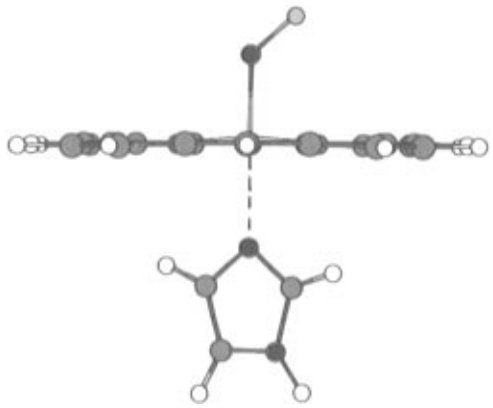

**Figure 11.** Ground-state geometry of the FeP(Im)(NO) complex. The weak bond to the imidazole ligand is represented by a dashed line. The orientation of the N−O axis with respect to the N-plane is very similar to that of Figure 10b, with the N−O axis projection slighly closer to one of the Fe−N distances.

in the FeP(Im)($O_2$) and FeP(Im)(CO) complexes, by the same method we used in the FeP($O_2$) structure. The results, reported in Table 3, show that our model is able to reproduce the slowing down of the O−O stretching associated with the strengthening of the competing Fe−O bond. The results for the CO stretching frequency in the FeP(Im)(CO) complex also agree with the experimental frequencies.

**The FeP(Im)(NO) Complex.** The simultaneous complexation of FeP by NO and Im is of considerable interest, because experimental results[42b,45] show that NO reduces the binding of Im to an iron−porphyrin derivative. The same *trans-repulsive* effect has been invoked to explain structural rearrangements in heme proteins such as guanylate cyclase.[45] The structure resulting from our geometry optimization has the iron atom almost in the porphyrin plane ($d$ = 0.09 Å), longer Fe−NO and N−O distances (1.72 and 1.20 Å, respectively) than FeP(NO), and a more pronounced Fe−N−O bending ($\Theta$ = 138°). The porphyrin core loses completely its domed shape characteristic of the five-coordinated complexes, as can be appreciated in Figure 11. More apparent is the change in the Fe−Im bond, which now shows a Fe−$N_\epsilon$ distance of 2.22 Å, i.e., 0.15 Å longer than the FeP(Im)($O_2$) and FeP(Im)(CO) complexes and 0.08 Å longer than in FeP(Im). Our computed FeP(Im)(NO) structure is in good agreement with the experimental data of ref 42b (see also Table 5). Consist with the fact that Im is almost displaced by the binding of NO, the strength of the Fe−NO bond in FeP(Im)(NO) (36 kcal/mol) is almost equal to that of FeP(NO) (35 kcal/mol). The binding of Im to FeP, on the other hand, is weakened: the energy required to break FeP(NO)(Im) into FeP(NO) and Im is slightly less than 6 kcal/mol, while in FeP(Im)($O_2$) and FeP(Im)(CO) it amounts to 12 kcal/mol. Prompted by the observation of different EPR spectra at $T$ = 77 K and $T$ = 300 K,[41,46] we investigated the structural dependence of FeP(NO)(Im) on temperature. To this aim, we performed a short MD simulation of an isolated $^2$FeP(NO)(Im) complex at 300 K. As expected, the Fe−N−O angle displays large-amplitude oscillations, since the angular restoring force is very weak. More importantly, the motion of NO around Fe is highly anharmonic. Apart from the structure of the Fe−N−O fragment, the other features of the complex (including the average Fe−$N_\epsilon$ distance) do not change significantly from 0 to 300 K. Although our simulation does not provide a direct explanation of the experiments (the observed drastic change of EPR spectra in raising the temperature from 77 to 300 K), a strong dependence of the Fe−N−O geometry on temperature is highlighted. A more detailed study of the effect of the temperature on the structure and electronic properties of FeP(Im)(NO) is in progress.

## VIII. Final Remarks

Density functional theory has been applied to the study of the FeP molecule and two series of FeP-based complexes: the five-coordinated FeP(A), with A = $O_2$, CO, NO, and Im, and the six-coordinated FeP(Im)(B), with B = $O_2$, CO, and NO. Our computations provide for the first time a consistent set of data for binding energies and electronic properties that allow us to understand trends and relations between the structure and chemical activity for this family of molecules closely related to the heme group.

The properties of the CO, NO, and $O_2$ complexes turn out to be determined mainly by the energy and occupation of the frontier orbital ($\pi_g^*$) in the diatomic ligands. In the case of CO, the $\pi_g^*$ orbital is empty and remains at high energy upon formation of the Fe−CO bond. A linear Fe−C−O configuration optimizes the $\sigma$-bonding, as well as the $\pi$-back-bonding between iron and CO. These two features explain both the linear Fe−C−O geometry resulting from our simulation and the relatively high stability of the complex (26 kcal/mol). On the other extreme is the FeP($O_2$)complex. In this case the $\pi_g^*$ orbitals of $O_2$ lie at lower energy and are occupied by two electrons. Their bonding with FeP results in the occupation of an additional MO that is strongly antibonding for a linear Fe−O−O configuration, thus explaining the bent ground-state geometry obtained in our computation. We observe that one electron is transferred from iron to one of the $\pi_g^*$ orbitals of $O_2$. The remaining unpaired electron on $\pi_g^*$ is anti-ferromagnetically coupled to one unpaired spin on the d−$\pi$ orbitals on Fe, resulting in an open shell singlet.

This type of bonding corresponds well to the $Fe^{III}-O_2^-$ picture of Weiss. Molecular levels are filled up to the antibonding states of $O_2$, and the binding energy of the complex is rather low (9 kcal/mol).

In many respects, the most intriguing case is FeP(NO), since NO has an electronic structure intermediate between that of CO and that of $O_2$. The $\pi_g^*$ orbital of NO is close in energy to the HOMO of FeP, giving rise to an important hybridization of the molecular states. The binding of NO is the strongest of the series (35 kcal/mol), and the Fe−N−O angle (150°) is intermediate between the linear FeP(CO) and the geometry of FeP($O_2$). The unpaired spin is fully localized on iron, while NO supports an almost sinusoidal spin wave that integrates to zero spin. The FeP(NO) complex is the only one having, in addition to the $M = 2$ ground state, a spin excited state ($M = 4$) that is strongly bound (20 kcal/mol). The $M = 4$ species seems to be given by the anti-ferromagnetic coupling of the almost unperturbed $^2$NO with $^5$FeP. The presence of two spin multiplicities separated by rather low energy, together with the floppy and anharmonic dynamics of the Fe−NO unit, might be the reason for the anomalous EPR spectrum measured for this complex.

The addition of the Im ligand affects substantially the energy splitting of the FeP spin states, and we find that this effect is enhanced by small variations in the out-of-planarity of the Fe atom. In this respect, we suggest that the proximal histidine could easily control the electronic structure of the active center in heme proteins. The presence of the imidazole enhances the stability of the $O_2$ and CO complexes (15 kcal/mol in FeP(Im)($O_2$) and 35 kcal/mol in FeP(Im)(CO)). Once again, the NO complex behaves in an exceptional way: the addition of NO to FeP(Im) almost breaks the Fe−Im bond, resulting in a very long Fe−$N_\epsilon$ distance. The Fe−NO bond, having turned away the competing Im, has almost the same strength as in FeP(NO). This drastic weakening of the Fe−Im bond may provide a mechanism for structural rearrangement of the heme with respect to the protein framework.

Comparison of our optimized structures with the results for crystallized proteins shows that the FeP(Im)($O_2$) complex is almost unchanged by incorporation in myoglobin, while FeP(Im)(CO) is significantly distorted (in particular, the Fe−C−O angle and the Fe−C distance) by the protein environment. The importance of angular distortion of the Fe−(CO) unit has been analyzed by performing explicit computations for the energy required to bend the Fe−C−O bond (both in the presence and in the absence of Im). The results show that thermal energy alone is sufficient to produce the deviations from linearity (∼7°) observed for heme−proteins in solution. Much larger deformations (on the order of 30°) are required to affect significantly the stability of the FeP(CO) complex or, at least, to shift the relative stability of FeP(CO) with respect to FeP($O_2$).

**Acknowledgment.** We acknowledge the I.D.R.I.S. institute (Orsay, France) and Garching Computer Center (Garching, Germany) for providing the computational support. C.R. thanks the financial support of the "Training and Mobility of Researchers" program of the European Union under Contract No. ERBFMBICT96-0951.

## References and Notes

(1) See, for instance: (a) Dolphin, D. *The Porphyrins*; Academic Press: New York, 1978−1979; Vols. 1−7. (b) In *Structure and Bonding*; Springer-Verlag: Berlin, Vol. 64, 1987; Vol. 74, 1991; Vol. 84, 1995, and references therein. (c) Momenteau, M.; Reed, C. A. *Chem. Rev.* **1994**, *94*, 659.

(2) Kaim, W.; Schwederski, B. *Bioinorganic Chemistry: Inorganic Elements in the Chemistry of Life*; J. Wiley and Sons: New York, 1994.

(3) Stryer, L. *Biochemistry*, 4th ed.; Freeman: New York, 1995, p 152.

(4) (a) Yang, F; Phillips, G. N., Jr. *J. Mol. Biol.* **1996**, *256*, 762. (b) Schlichting, I.; Berendzen, J.; Phillips, G. N., Jr.; Sweet, R. M. *Nature* **1994**, *371*, 808. (c) Kuriyan, J.; Wilz, S.; Karplus, M.; Petsko, G. A. *J. Mol. Biol.* **1986**, *192*, 133. (d) Quillin, M. L. Arduini, R. M.; Olson, J. S.; Phillips, G. N. *J. Mol. Biol.* **1993**, *234*, 140. (e) Cheng, X.; Schoenborn, B. P. *J. Mol. Biol.* **1991** *220*, 381. (f) Phillips, S. E.; Shoenborn, B. P. *Nature* **1981**, *292*, 81. (g) Phillips, S. E. *J. Mol. Biol.* **1980**, *142*, 531.

(5) Service, R. F. *Science* **1995**, *269*, 921.

(6) (a) Matsuzawa, N.; Ata, M.; Dixon, D. A. *J. Phys. Chem.* **1995**, *99*, 7698. (b) Delley, B. *Physica B* **1991**, *172*, 185. (c) Obara, S.; Kashiwagi, H. *J. Chem. Phys.* **1982**, *77*, 3155.

(7) See, for instance: (a) Case, D. A.; Huynh, B. H.; Karplus, M. *J. Am. Chem. Soc.* **1979**, *101*, 4433. (b) Kirchner, R. F.; Loew, G. H. *J. Am. Chem. Soc.* **1977**, *99*, 4639. (c) Newton, J. E.; Hall, M. B. *Inorg. Chem.* **1984**, *23*, 4627. (d) Loew, G. H.; Kirchner, R. F. *Int. J. Quantum Chem. Quantum Biol. Symp.* **1978**, *5*, 403. (e) Doetschman, D. C. *Chem. Phys.* **1980**, *48*, 307. (f) Waleh, A.; Ho, N.; Chantranupong, L.; Loew, G. H. *J. Am. Chem. Soc.* **1989**, *111*, 2767. (g) Edwards, W. D.; Weiner, B.; Zerner, M. C. *J. Am. Chem. Soc.* **1986**, *108*, 2196.

(8) Hoffmann, R.; Chen, M. M.-L.; Thorn, D. *Inorg. Chem.* **1977**, *16*, 503.

(9) (a) Dedieu, A.; Rohmer, M.-M.; Benard, M.; Veillard, A. *J. Am. Chem. Soc.* **1976**, *98*, 3717. (b) Nakatsuji, H.; Hasegawa, J.; Ueda, H.; Hada, M. *Chem. Phys. Lett.* **1996**, *250*, 379. (c) Yamamoto, S.; Kashiwagi, H. *Chem. Phys. Lett.* **1989**, *161*, 85

(10) (a) Jewsbury, P.; Yamamoto, S.; Minato, T.; Saito, M.; Kitagawa, T. *J. Phys. Chem.* **1995**, *99*, 12677. (b) Ghosh, A.; Bocian, D. F. *J. Phys. Chem.* **1996**, *100*, 6363.

(11) Harris, D.; Loew, G. H. *J. Am. Chem. Soc.* **1997**, *101*, 3959.

(12) Ghosh, A.; Almlof, J.; Lawrence, Q., Jr. *J. Phys. Chem.* **1994**, *98*, 5576. See also refs 6a, 6b, 10b, and 11c.

(13) See, for instance: (a) Galli, G.; Parrinello, M. In *Computer Simulation in Materials Science*; Pontikis, V., Meyer, M., Eds.; Kluwer: Dordrecht, 1991. (b) Car, R.; Parrinello, M. *Phys. Rev. Lett.* **1985**, *55*, 2471.

(14) (a) Carloni, P.; Andreoni, W. *J. Phys. Chem.* **1996**, *100*, 17797. (b) Marchi, M.; Hutter, J.; Parrinello, M. *J. Am. Chem. Soc.* **1996**, *118*, 7847. (c) Hutter, J.; Carloni, P.; Parrinello, M. *J. Am. Chem. Soc.* **1996**, *118*, 8710. (d) Sagnella, D. E.; Laasonen, K.; Klein, M. L. *Biophys J.* **1996**, *71*, 1172.

(15) (a) Lamoen, D.; Parrinello, M. *Chem. Phys. Lett.* **1996**, *248* 309. (b) Preliminary results on the $O_2$ and CO complexes of FeP are reported in: Rovira, C.; Ballone, P.; Parrinello, M. *Chem. Phys. Lett.* **1980**, *271*, 247.

(16) Parr, R. G.; Yang, W. *Density Functional Theory of Atoms and Molecules*; Oxford University Press: Oxford, 1989.

(17) We use the electron gas data of: Ceperley, D. M.; Alder, B. J. *Phys. Rev. Lett.* **1980**, *45*, 566, as interpolated by Perdew, J. P.; Zunger, A. *Phys. Rev. B* **1981**, *23*, 5048.

(18) (a) Becke, A. D. *J. Chem. Phys.* **1986**, *84*, 4524. (b) Perdew, J. P. *Phys. Rev. B* **1986**, *33*, 8822. (c) Lee, C.; Yang, W.; Parr, R. G. *Phys. Rev. B* **1988**, *37*, 785.

(19) (a) Troullier, N.; Martins, J. L. *Phys. Rev. B* **1991**, *43*, 1993. (b) See: Pickett, W. A. *Comput. Phys. Rep.* **1989**, *9*, 115, for an overview of pseudopotential techniques in condensed matter physics.

(20) (a) Kleinman, L.; Bylander, D. M. *Phys. Rev. Lett.* **1982**, *48*, 1425. (b) Louie, S. G.; Froyen, S.; Cohen, M. L. *Phys. Rev. B* **1982**, *26*, 1738.

(21) The transferability of spin excitation energies is discussed in: Ballone, P.; Jones, R. O. *Chem. Phys. Lett.* **1995**, *233*, 632.

(22) Computations have been performed by the CPMD program version 3.0, written by J. Hutter, Max-Planck-Institut für Festkörperforschung, Stuttgart, 1996.

(23) (a) Stich, I.; Car, R.; Parrinello, M.; Baroni, S. *Phys. Rev. B* **1989**, *39*, 4997. (b) Hutter, J.; Lüthi, H. P.; Parrinello, M. *Comput. Mater. Sci.* **1994**, *2*, 244.

(24) The atomic coordinates of our optimized structures are available by anonimous ftp (address: parrix1.mpi-stuttgart.mpg.de, directory pub/outgoing/fep).

(25) We estimate the uncertainty on bond distances within 0.02 Å and on binding energies about 1 kcal/mol. These estimates refer to the numerical accuracy of the computation within the DFT−LDA+GC scheme. Deviations from experiment may be slightly larger, because of approximations implicit in our method and because experiments are done on crystal structures, while our computations are performed on molecules.

(26) Mayer, I. *Chem. Phys. Lett.* **1983**, *97*, 270.

(27) We project on the pseudoatomic 1s orbital of H, (2s, 2p) of C, N, and O, and (3d, 4s, 4p) of Fe.

(28) (a) Kobayashi, H.; Maeda, Y. Yanagawa, A. *Bull. Chem. Soc. Jpn.* **1970**, *43*, 2342. (b) Lang, G.; Spartalian, K.; Reed, C. A.; Collman, L. *J. Chem. Phys.* **1978**, *69*, 5424. (c) Goff, H.; La Mar, G. N.; Reed, C. A. *J. Am. Chem. Soc.* **1977**, *77*, 3641. (d) Collman, J. P.; Hoard, J. L.; Kim, N.; Lang, G.; Reed, C. A. *J. Am. Chem. Soc.* **1975**, *97*, 2676.

(29) Small deviations from the $D_{4h}$ symmetry were found for the triplet state, which might suggest a symmetry reduction by means of a Jahn−Teller mechanism. Nevertheless, the magnitude of the distortion is within the uncertainties of our structural determination.

(30) Scheidt, W. R.; Reed, C. A. *Chem. Rev.* **1981**, *81*, 543.
(31) See for instance: Albrigth, T. A.; Burdett, J. K.; Whangbo, M.-H. *Orbital Interactions in Chemistry*; John Wiley: New York, 1985.
(32) (a) Weiss, J. J. *Nature* (*London*) **1964**, *202*, 83. (b) Pauling, L.; Coryell, C. D. *Proc. Natl. Acad. Sci. U.S.A.* **1936**, *22*, 210.
(33) (a) Watanabe, T.; Ama, T.; Nakamoto, K. *J. Phys. Chem.* **1984**, *88*, 440. (b) Proniewicz, L. M.; Paeng, I. R.; Nakamoto, K. *J. Am. Chem. Soc*. **1991**, *113*, 3294. (c) Nakamoto, K. *Coord. Chem. Rev.* **1990**, *100*, 363.
(34) Gubelmann, M. H.; Williams, A. F. *Struct. Bonding* **1983**, *55*, 1.
(35) The bend and tilt modes of $O_2$ are at much lower frequency and therefore are uncoupled from the stretching mode.
(36) Kutzler, F. W.; Painter, G. S. *Phys. Rev. B* **1992**, *45*, 3236.
(37) Lim, M.; Jackson, T. A.; Anfirud, P. A. *Science* **1995**, *269*, 962.
(38) Additional calculations performed including an imidazole axial ligand result in a very similar bending potential (for a bending of 10°, a sligthly lower deformation energy of 1 kcal/mol was obtained).
(39) (a) Peng, S.-M.; Ibers, J. A. *J. Am. Chem. Soc.* **1976**, *98*, 8032. (b) Kim, K.; Ibers, J. A. *J. Am. Chem. Soc.* **1991**, *113*, 6077. (c) Kim, K.; Fettinger, J.; Sessler, J. L.; Cyr, M.; Hugdahl, J.; Collman, J. P.; Ibers, J. A. *J. Am. Chem. Soc.* **1989**, *111*, 403. (d) Ray, G. B.; Li, X.-Y.; Ibers, J. A.; Sessler, J. L.; Spiro, T. G. *J. Am. Chem. Soc.* **1994**, *116* 162.
(40) Springer, B. A.; Sligar, S. G.; Olson, J. S.; Phillips, J. N., Jr. *Chem. Rev.* **1994**, *94*, 699.
(41) (a) Kon, H. *J. Biol. Chem.* **1968**, *243*, 4350. (b) Chien, J. C. W. *J. Chem. Phys.* **1969**, *51*, 4220. (c) Dickinson, L. C.; Chien, J. C. W. *J. Am. Chem. Soc.* **1971**, *93*, 5036. (d) Hori, H.; Ikeda-Saito, M.; Yonetani, T. *J. Biol. Chem.* **1981**, *256*, 7849.
(42) (a) Scheidt, W. R.; Frisse, M. E. *J. Am. Chem. Soc.* **1975**, *97*, 17. (b) Scheidt, W. R.; Piciulo, P. L. *J. Am. Chem. Soc.* **1976**, *98*, 1913.
(43) (a) The bond lengths for the gas-phase NO, $NO^+$, and $NO^-$ are the following. $^2$NO: $r_e = 1.17$ Å (expt = 1.15 Å). $^1NO^-$: $r_e = 1.22$ Å (expt = 1.26 Å). $NO^+$: $r_e = 1.08$ Å (expt = 1.06 Å). (b) Stamler, J. S.; Singel, D. J.; Loscalzo, J. *Science* **1992**, *258*, 1898.
(44) (a) Jameson, G. B.; Rodley, G. A.; Robinson, W. T.; Gagne R. R.; Reed, C. A.; Collman, J. A. *Inorg. Chem.* **1978**, 17, 850. (b) Jameson, G. B.; Molinaro, F. S.; Ibers, J. A.; Collman, J. P.; Brauman, J. I.; Rose, E.; Suslick, K. S. *Inorg. Chem.* **1980** *102*, 3224.
(45) Traylor, T. G.; Vijay S. *Biochemistry* **1992** *31*, 2847.
(46) Morse, R. H.; Chan, S. I. *J. Biol. Chem.* **1980**, *255*, 7876.
(47) Hirota, S.; Ogura, T.; Shinzawa-Itoh, K.; Yoshikawa, S.; Nagai, M.; Kitagawa, T. *J. Phys. Chem.* **1994**, *98*, 6652.
(48) (a) Herzberg, G. *Molecular Spectra and Molecular Structure*; 2nd ed.; Van Nostrand: New York, 1950. (b) Huber, K. P. In *American Institute of Physics Handbook*; McGraw-Hill: New York, 1972; section 7g.